2.7 A WAY TO ESTIMATE THE PARAMETERS

The previous analysis on pool C_2 and C_3 can provide us with important information regarding τ_b/τ_1, τ_2/τ_1, and τ_3/τ_1 by just examing the transient response curves. To estimate the order of magnitude of these parameters, on the other hand, we developed the following method ($^{12}CO/^{13}CO$ exchange is assumed).

we first define the "area for $^{12}C_i{}^{13}C_{k-i}$" as

$$\text{Area for } {}^{12}C_i{}^{13}C_{k-i} \equiv \int_0^\infty {}^{k}F_{{}^{12}C_i{}^{13}C_{k-i}} \cdot dt \qquad (2\text{-}112)$$

i is the ^{12}C number in C_k molecules (can be any number from 1 to k).

for i = 0,

$$\text{Area for } {}^{13}C_k \equiv \int_0^\infty (1 - {}^{k}F_{{}^{12}C_i{}^{13}C_{k-i}}) \cdot dt \qquad (2\text{-}113)$$

The geometric representation of these two definitions is shown in Fig.2-15.

Since ${}^{k}F_i$ is dimensionless, the area for $^{12}C_i{}^{13}C_{k-i}$ has the unit of time.

Dividing both sides of Eq.2-112 and 2-113 by τ_1, we obtain dimensionless groups:

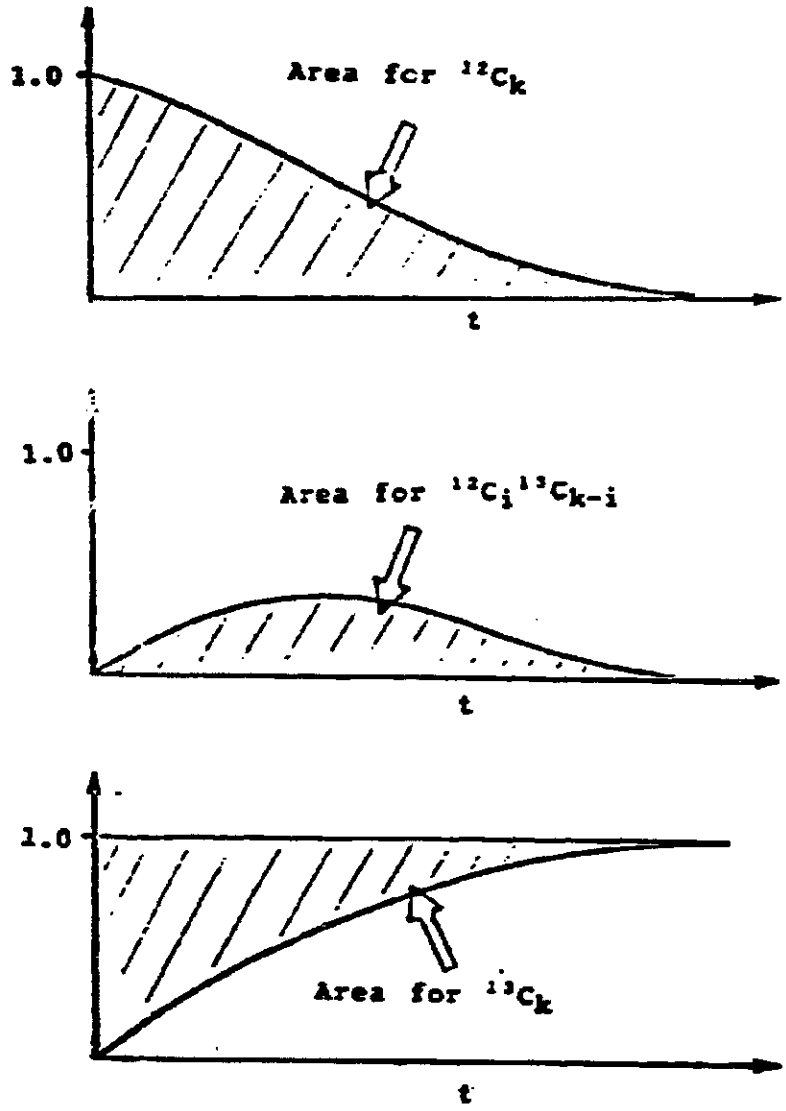

Figure 2-15: The Geometric Representation of the Definitions 2-112 and 2-113

(Area for $^{12}C_i{}^{13}C_{k-i}$)/τ_1

$$\equiv \int_0^\infty {}^{k}F_{^{12}C_i{}^{13}C_{k-i}} \cdot d(t/\tau_1) \qquad (2\text{-}114)$$

and

$$(\text{Area for } {}^{13}C_k)/\tau_1 \equiv \int_0^\infty (1-{}^{k}F_{^{12}C_i{}^{13}C_{k-i}}) \cdot d(t/\tau_1) \qquad (2\text{-}115)$$

From Appendix A, it is readily seen that, when assuming $\tau_0 = 0$ (a fact that has been verified from experiment),

$${}^{k}F_{^{12}C_i{}^{13}C_{k-i}} = {}^{k}f_i(t/\tau_1, \tau_b/\tau_1, \ldots, \tau_k/\tau_1) \qquad (2\text{-}116)$$

and

$${}^{k}F_{^{13}C_k} = {}^{k}f_0(t/\tau_1, \tau_b/\tau_1, \ldots, \tau_k/\tau_1) \qquad (2\text{-}117)$$

Here a superscript ^{k} means pool C_k, a subscript $_i$ means species $^{12}C_i{}^{13}C_{k-i}$.

Substituting Eq.2-116 and 2-117 into Eq.2-114 and 2-115, respectively, we obtain, in general form,

(Area for $^{12}C_i{}^{13}C_{k-i}$)/τ_1

$$= {}^{k}g_i(\tau_b/\tau_1, \ldots, \tau_k/\tau_1) \qquad (2\text{-}118)$$

and

(Area for $^{13}C_k$)/τ_1

$$= {}^{k}g_0(\tau_b/\tau_1, \ldots, \tau_k/\tau_1) \qquad (2\text{-}119)$$

For k=1,

$$^{1}F_{1,2_C} = {}^{1}f_1(t/\tau_1) \qquad (2\text{-}120)$$

and

$$^{1}F_{1,3_C} = {}^{1}f_0(t/\tau_1) \qquad (2\text{-}121)$$

Therefore, substituting Eq.2-120 and 2-121 into Eq.2-114 and 2-115, respectively, yields,

$$(\text{Area for } {}^{12}C_1)/\tau_1 = 1 \qquad (2\text{-}122)$$

and

$$(\text{Area for } {}^{13}C_1)/\tau_1 = 1 \qquad (2\text{-}123)$$

for k=2, 3, we obtain the following expressions from Eq.2-118 and 2-119:

$$(\text{Area for } {}^{12}C_2)/\tau_1 = {}^{2}g_2(\tau_b/\tau_1,\ \tau_2/\tau_1) \qquad (2\text{-}124)$$

$$(\text{Area for } {}^{12}C_1{}^{13}C_1)/\tau_1 = {}^{2}g_1(\tau_b/\tau_1,\ \tau_2/\tau_1) \qquad (2\text{-}125)$$

$$(\text{Area for } {}^{13}C_2)/\tau_1 = {}^{2}g_0(\tau_b/\tau_1,\ \tau_2/\tau_1) \qquad (2\text{-}126)$$

$$(\text{Area for } {}^{12}C_3)/\tau_1 = {}^{3}g_3(\tau_b/\tau_1,\ \tau_2/\tau_1,\ \tau_3/\tau_1) \qquad (2\text{-}127)$$

$$(\text{Area for } {}^{12}C_2{}^{13}C_1)/\tau_1 = {}^{3}g_2(\tau_b/\tau_1,\ \tau_2/\tau_1,\ \tau_3/\tau_1) \qquad (2\text{-}128)$$

(Area for $^{12}C_1{}^{13}C_2)/\tau_1$

$$= {}^3g_1(\tau_b/\tau_1,\ \tau_2/\tau_1,\ \tau_3/\tau_1) \qquad (2\text{-}129)$$

(Area for $^{13}C_3)/\tau_1$

$$= {}^3g_0(\tau_b/\tau_1,\ \tau_2/\tau_1,\ \tau_3/\tau_1) \qquad (2\text{-}130)$$

For a choosen set of parameters (τ_1, τ_b/τ_1, τ_2/τ_1, τ_3/τ_1), we can calculate the area's with expressions for Eq.2-124 through 2-130. A plot of (Area for $^{12}C_i{}^{13}{}_{k-i}$ / τ_1) vs τ_k/τ_1 at constant τ_j/τ_1 (j=b,2,...,k-1) can then be made as those shown in Appendix D.

In general, we can calculate the area for $^{12}C_i{}^{13}{}_{k-i}$ from the transient experimental data. Next, Eq.2-122 is used for estimating τ_1, whereas Eq.2-123 is to check whether the same τ_1 can be obtained. Thus, the leftside of Eq.2-124 through 2-130 are determined. Any two of Eq.2-124 through 2-126 can be used to determine τ_b/τ_1 and τ_2/τ_1, the remaining one is used for checking. Any three of Eq.2-127 through 2-130 can be used to determine τ_b/τ_1, τ_2/τ_1 and τ_3/τ_1, the remaining one is for checking. The parameters τ_b/τ_1 and τ_2/τ_1 obtained from Eq.2-127 through 2-130 can be compared with those obtained from Eq.2-124 through 2-126 to check whether they are consistent.

In practical, because of the complexity of the real situation, larger errors in estimating parameters could be expected with the above method. The advantage of the above

method lies in that it can easily provide us with a range in which parameters may be expected. We should use the computer simulation to check whether we obtained correct parameters from the above method. If the parameters are correct, the computer simulation should feature the experimental data such as the maximum of ${}^2F^{13}C_1^{12}C_1$ and the simultaneous rising feature (Section 5.2).

2.8 SUMMARY

When we look at a transient experimental data, the first question we may ask is "did we observe τ_2 and τ_3?". we can check it by simply examing the transient data with the method developed in Section 2.5 and 2.6.

Theoretically, since the area's are functions of multiparameters, τ_b, τ_1, τ_2, etc, it is possible that two different sets of τ's result in essentially the same area's in computer simulation. In fact, we do find that area's at $\tau_b/\tau_1 \ll 1$ and $\tau_2/\tau_1 = \tau_3/\tau_1 \approx 1$ is around the same as at $\tau_b/\tau_1 \approx 1$ and $\tau_2/\tau_1 = \tau_3/\tau_1 \ll 1$. By using the criteria in Section 2.5, we may immediately discriminate between alternatives, which can, to a large extent, decrease the amount of work in data analysis.

Then, the estimated τ's are to be substituted into expressions for transient responses to see if they feature the experimental data.

CHAPTER 3.0

EXPERIMENTAL

3.1 PREPARATION OF THE CATALYSTS

(1) Unsupported Co_2O_3 was prepared by precipitation from a 0.5 m cobalt (II) nitrate solution by concentrated ammonium hydroxide (25% NH_3)([10]). The suspension was heated to 110°C. The blue precipitate was filtered off and washed five times with distilled water. The catalyst was dried at 120°C for 16 hr and calcined at 450°C for 1 hr. Then it was mixed with SiO_2 beads (mesh size 150 - 70), in a ratio of 1:1. This SiO_2-beads-supported-Co_2O_3 was reduced at 350°C for 12 hr in flowing hydrogen (8 nl/hr)**. According to XRD, the finished catalyst consisted of hexagonal α-cobalt exclusively. It has an exposed cobalt surface area equivalent to 1 ml (stp) CO / g catalyst, as determined from $^{12}CO/^{13}CO$ exchange, at 100°C.

(2) Ru/Al_2O_3 was prepared by dry impregnation with $RuCl_3$. Reduction was carried out in flowing hydrogen at 300°C for 2 h. The finished catalyst has an exposed ruthenium surface area equivalent to 5 ml (stp) CO/g catalyst, as determined from $^{12}CO/^{13}CO$ exchange at 100°C.

**We acknowledge the supply of the Co-based catalyst by Mr. Gormly, Pittsburgh Energy and Technol. Center

3.2 EQUIPMENT AND EXPERIMENTAL PROCEDURE

The transient experiments were carried out in a differential reactor with internal diameter of 4.5 mm. Gas transfer lines associated with the reactor are typically 1.4 mm ID stainless steel tubing. The reactor outlet is connected to a mass spectrometer via a 1 meter length heated stainless steel capillary (0.1mm ID) transfer line and a Varian flow-by leak valve, pumped by a Balzer's 40 l/s turbomolecular pump. The Extra Nuclear 2750-50 quadrupole mass spectrometer is being housed in a permanently baked (100°C) UHV-compatible vacuum chamber. The intensities of selected masses are collected continuously with a micro-computer.

3.3 THE CHOICE OF MS PEAKS

The mass spectrum of a compound contains the masses of the ion fragments. For hydrocarbons under investigation (C_2 and C_3), three fragments are usually observed, as shown in Fig.3-1.

If H_2 is used to react with ^{12}CO, these three fragments are 27, 28, 29 for C_2 and 41, 42, 43 for C_3. When switching from ^{12}CO to ^{13}CO, the fragments become 29, 30, 31 for C_2 and 44, 45, 46 for C_3. There are two difficulties in detecting them:

First, mass 28 and 29 are also fragments for ^{12}CO and ^{13}CO. Usually, the intensities of $^{12}C^-$ and ^{13}CO are much

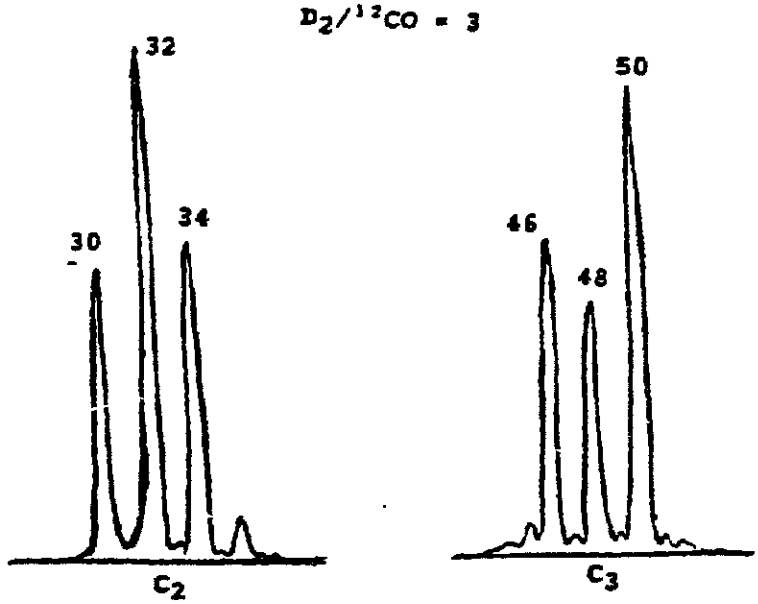

Figure 3-1: Mass Spectrum for C_2 and C_3

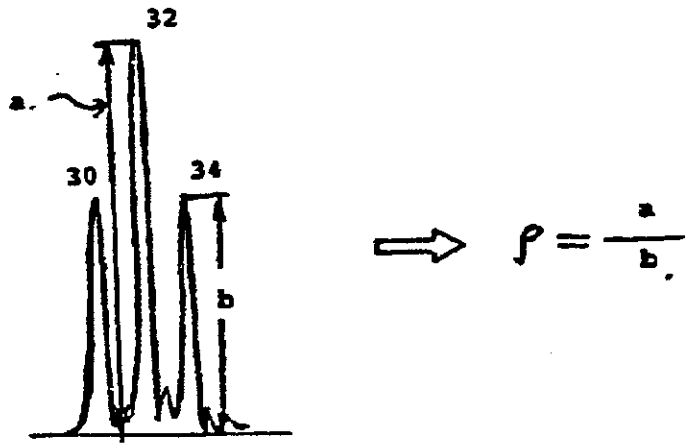

Figure 3-2: A Way to detect $^{12}C_2$

larger than that of C_2. Therefore, mass 28 is not sensitive to the change in C_2. Furthermore, a big peak in mass 28 may overshadow its neighboring (mass 27 and 28). For these reasons, the change in $^{12}C_2$ is very difficult to be observed.

Secondly, it is hard to detect intermediates like $^{12}C_1{}^{13}C_2$ and $^{12}C_2{}^{13}C_1$ because the fragments of these compounds are overlapped. In order to find the transient change of these intermediates, a knowledge of the mass spectrum of each compound is required since the spectrum of the mixture is the sum of the individual spectra. But, unfortunately, there is a shortage of data because of the unavailability of pure standard compounds like $^{12}C_2{}^{13}C_1H_6$ and $^{12}C_1{}^{13}C_2H_6$.

Instead of using H_2, we choose D_2 to react with CO. Three fragments are 30, 32, 34 for $^{12}C_2$ and 46, 48, 50 for $^{12}C_3$. When switching from ^{12}CO to ^{13}CO, the fragments become 32, 34, 36 for $^{13}C_2$ and 49, 51, 53 for $^{13}C_3$.

It can be readily seen that there is no overlap on mass 46, 47, 52, and 53 which are the fragments of $^{12}C_3$, $^{12}C_2{}^{13}C_1$, $^{12}C_1{}^{13}C_2$ and $^{13}C_3$. We can just observe these masses, assuming the transient response in one fragment of a compound is the same for other fragments of the same compound.

Mass 36 and 33 can be selected to detect the peaks in

$^{13}C_2$ and $^{12}C_1{}^{13}C_1$. Theoretically, mass 30 can be used to detect $^{12}C_2$. However, since mass 29 is much larger one (^{13}CO), mass 30 can not be detected while doing transient experiment, which forces us to consider other fragments of $^{12}C_2$. As the mass 30 is the only fragment of $^{12}C_2$, the detection of other fragments will have to deal with the overlapping problem. The mass we chose is 34. The following method is used to find the change in $^{12}C_2$ (see Fig.3-2).

1. The steady state intensities of mass 32 and 34, flowing with ^{12}CO and D_2, were measured. The ratio of the intensity of mass 32 over 34 is designated as ρ.

2. While switching from ^{12}CO to ^{13}CO, assuming the fragment pattern remains unchangeable, then the intensity due to $^{12}C_2$ is related to the intensities of mass 34 and 36 as follows:

$$I_{^{12}C_2} = I^{34} - \rho \cdot I^{36} \qquad (3\text{-}1)$$

where,

$I_{^{12}C_2}$ is the intensity due to $^{12}C_2$.

I^{34} and I^{36} are the intensities of mass 34 and 36.

Within experimental error, this way of detecting $^{12}C_2$ does lead to $\sum^{2} F_{12} {}^{12}C_i {}^{13}C_{2-i} = 1$, a condition to be met with for all correct detection of $^{12}C_2$.

3.4 CONDITIONS

The experiments were carried out under the following conditions:

$T = 210^{\circ}C$

$P = 1$ atm

$D_2/CO = 1 - 6.6$

CO flow rate = 0.3 - 0.6 nl/h

CHAPTER 4.0

RESULTS

Fig.4-1 gives the response curve for switching the reactant stream at the reaction temperature from (0.004 bar Ar, 0.18 bar ^{12}CO, 0.54 bar D_2) towards (0.18 bar ^{13}CO, 0.54 bar D_2). On the vertical axis are the ion currents at m=28 (^{12}CO), m=29 (^{13}CO), m=40 (Ar), and m=21 ($^{13}CD_4$), divided by their respective steady state values measured well before (Ar, ^{12}CO) or after the switch (^{13}CO). Therefore, the quantity on the vertical axis is a dimensionless fraction F, varing between 0.0 and 1.0. The horizontal axis is the time in seconds.

Ru is a very active catalyst. The situation in Fig.4-2 shows that the lifetime for the C_1 intermediate is very small (within 2 sec)([6]). The experiment also shows that $F^{13}C$ in C_3 is identical to $^1F^{13}C$. Because of the limitation of the instrument precision, the fast reaction on Ru catalyst prevents us from obtaining further information.

On the contrary, Co catalyst is not as active as Ru. The lifetime for C_1 is around 20 sec. Therefore, information regarding the FT mechanism over Co catalyst can be obtained. The following is the result.

Upon replacement of $^{12}CO/Ar$ by $^{13}CO/Ar$ there is

continuing production of $^{13}CD_4$. This production is fed by ^{13}C-containing surface intermediates, which is gradually increasing after $^{12}CO/^{13}CO$ switch (c.f. Fig.4-1).

Data with regard to C_2 and C_3 are demonstrated in Fig.4-3 and 4-4. Upon replacement of ^{12}CO by ^{13}CO, the production of $^{12}C_2$ and $^{12}C_3$ are continuously decreasing while the production of $^{13}C_2$ and $^{13}C_3$ are increasing (the ion currents at selected masses (Section 4-1) for $^{12}C_2$, $^{13}C_2$, $^{12}C_3$ and $^{13}C_3$ are normalized relative to their respective steady state values). For all the intermediates ($^{12}C_1{}^{13}C_1$, $^{12}C_1{}^{13}C_2$, $^{12}C_2{}^{13}C_1$) the production is increasing first and, after certain time, decreasing (the ion currents of $^{12}C_1{}^{13}C_1$ are normalized relative to the steady state value for $^{12}C_2$ and the ion currents of $^{12}C_1{}^{13}C_2$ and $^{12}C_2{}^{13}C_1$ are normalized to the steady state value of $^{12}C_3$).

With respect to Fig.4-3 and 4-4, some conclusions can be drawn here from the general study of the transient response curve given in Chapter 2:

(1) Theoretical study shows that if τ_2=0, the minimum value for the peak of $^2F^{12}C_1{}^{13}C_1$ is 0.5. Corresponding to this minimum value is that the lifetime for the C_1-building surface intermediate is the same as that for C_1 surface intermediate. Therefore, if $\tau_2 > 0$, only $\tau b < \tau_1$ can result in the situation where the time needed for the appearance of the peak is equal to that for $F^{13}C = 0.5$ and the peak is [illegible] than 0.5. The experimental data this situation

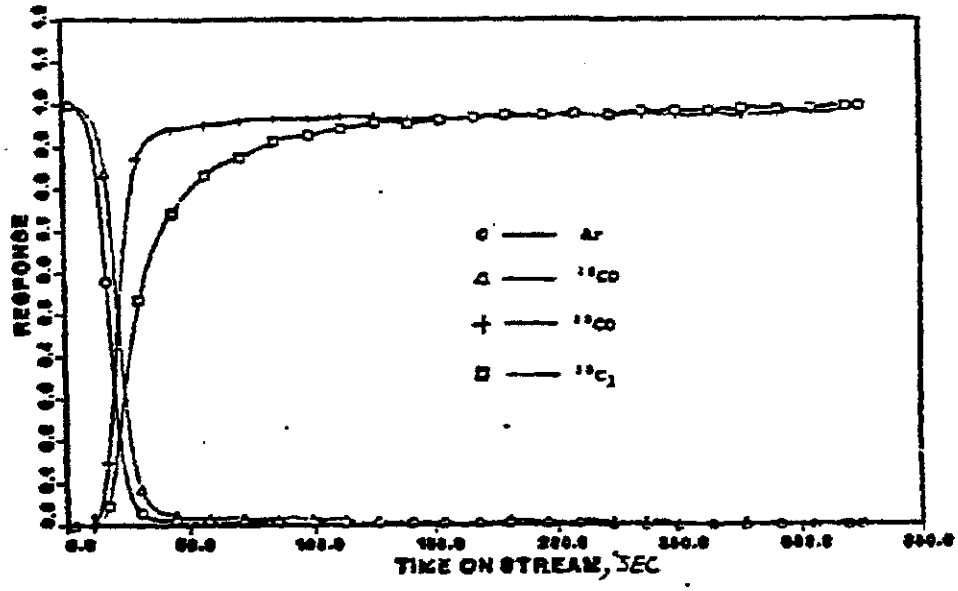

Figure 4-1: Transient experiment over Co catalyst: #1: ^{12}CO, ^{13}CO, $^{13}CD_4$ and Ar

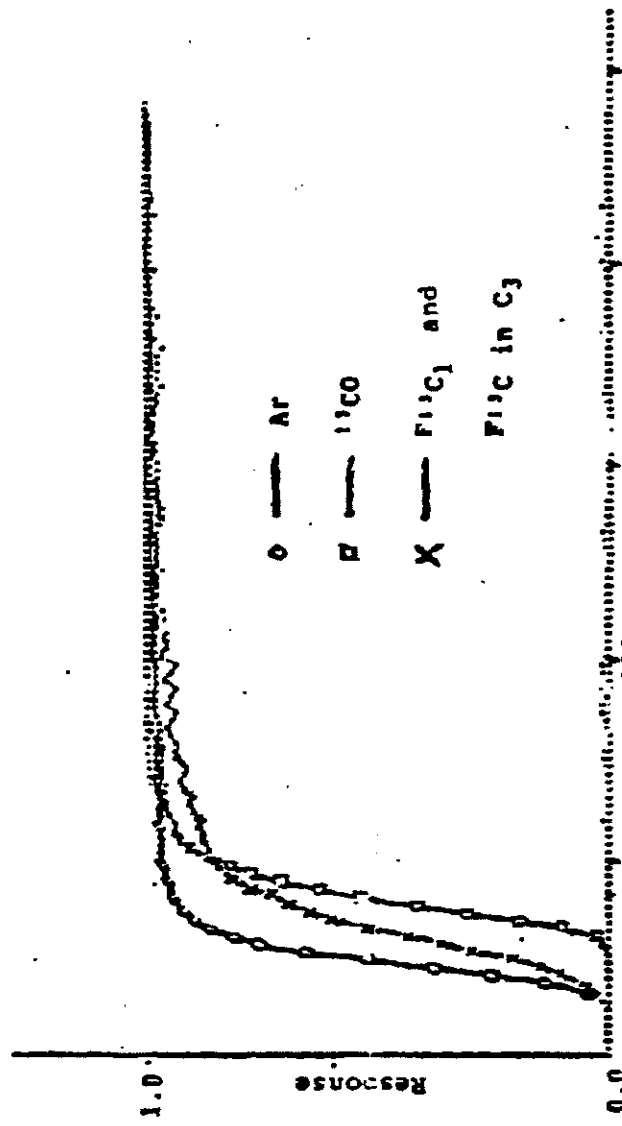

Figure 4-2: Transient experiment over Ru catalyst: ^{13}CO, $^{13}CD_4$, $F^{13}ClnC_3$ and Ar

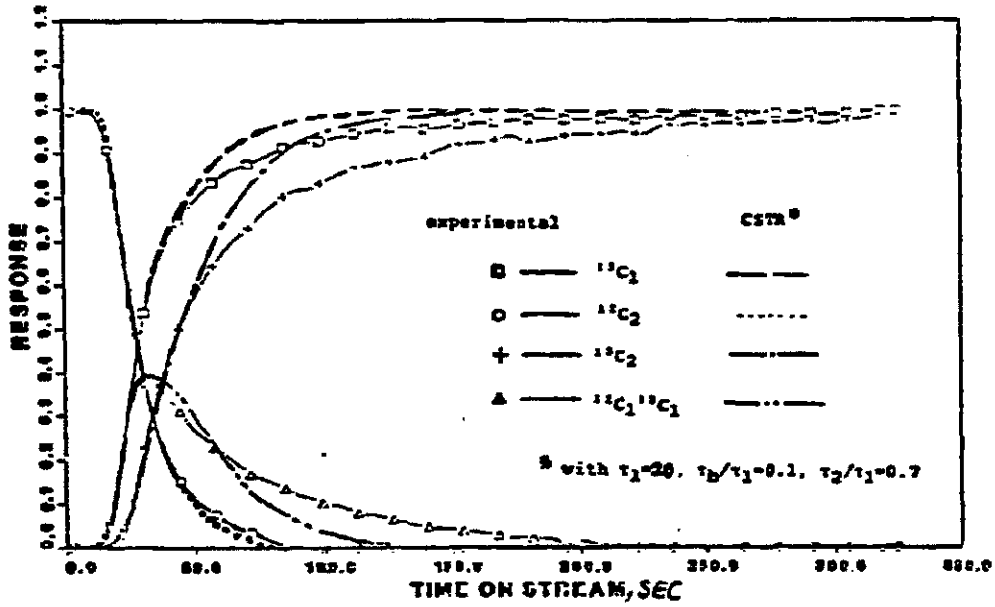

Figure 4-3: Transient Experiment over Co Catalyst #2: C_1 and C_2

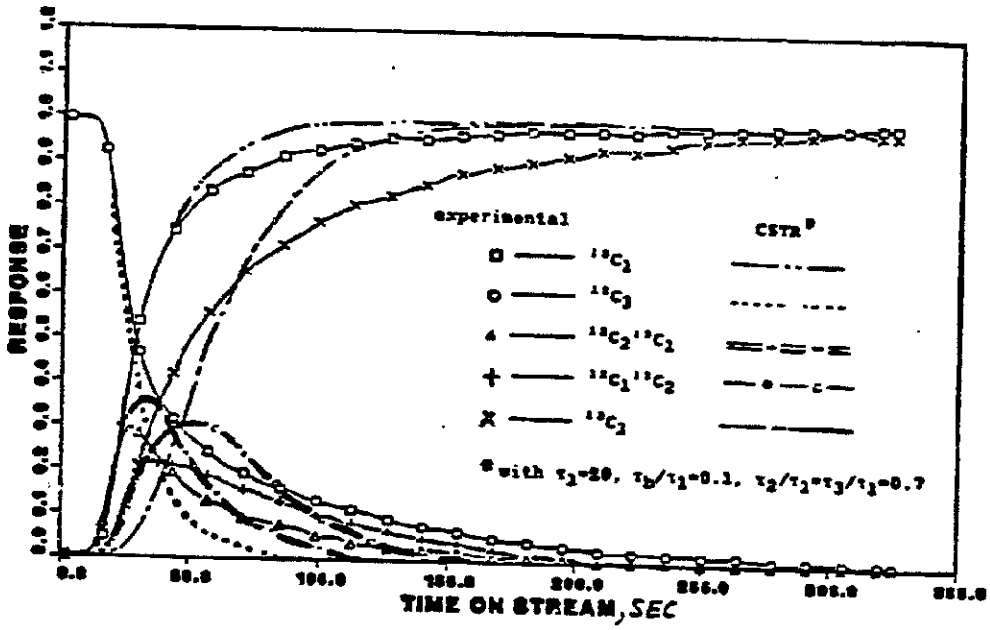

Figure 4-4: Transient Experiment over Co Catalyst #3: C_1 and C_3

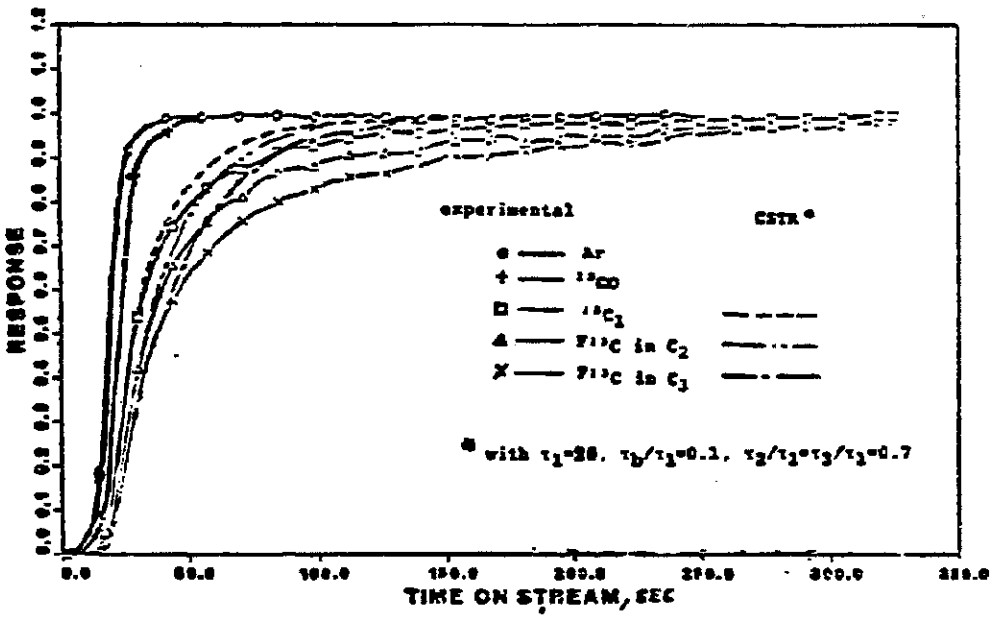

Figure 4-5: Transient Experiment over Co catalyst #4: Ar, CO, C_1, C_2 and C_3

Therefore, we can conclude that $\tau b < \tau_1$ and τ_2 is observable.

(2) The general study gives a criterion to judge whether τ_3 is observable (Section 2.7). Fig.4-5 is the plot of $F^{13}CinC_2$, $F^{13}CinC_3$ and $F^{13}C_1$, showing that $3(F^{13}CinC_2-F^{13}Cinc_3)$ is larger than $F^{13}C_1-F^{13}CinC_2$. It emerges, therefore, that the lifetime for C_3 surface intermediate is observable.

Utilizing the method developed in Section 2.7, we calculated the area for $^{12}C_i{}^{13}C_{k-i}$ (Table 4-1). An estimation of τ_1, τ_b/τ_1, τ_2/τ_1, and τ_3/τ_1 is accordingly found from the area vs τ plots (Appendix D) and the computer simulation.

For $D_2/CO = 3$, $CO = 0.45$ nl/h, the result is:

(1) Area vs τ plot method:

from area for C_1,

$\tau_1 = 20$ sec

from areas for C_2 species,

$\tau_b / \tau_1 = 0.01 \sim 0.20$

$\tau_2 / \tau_1 = 0.6 \sim 0.8$

from areas for C_3 species,

$\tau_b / \tau_1 = 0.01 \sim 0.20$

$\tau_2 / \tau_1 = 0.7 \sim 0.9$

$\tau_3 / \tau_1 = 0.8 \sim 1.2$

(2) Computer simulation:

$\tau_1 = 20$ sec, $\tau_b / \tau_1 = 0.1$,

$\tau_2 / \tau_1 = \tau_3 / \tau_1 = 0.7$

or

$\tau_b = 2$ sec, $\tau_2 = \tau_3 = 14$ sec

It should be noted that the computer simulation only features the experimental data approximately. Later in Chapter 5, we will look at the discrepancy between the predicted and the experimental data.

The effect of varing D_2/CO ratio on the areas for species C_1, C_2 and C_3 at the temperature 210°C has been investigated, as can be seen from Fig.4-6, 4-7 and 4-8.

Within the experimental error, it emerges that the activity of the intermediates in the range of D_2/CO=1 to 6.54 essentially does not change with D_2/CO ratio (τ_1 = 20 sec, τ_b = 2 sec, $\tau_2 = \tau_3$ = 14 sec). However, the TOF for CD_4 production increases with D_2 CO ratio (Fig.4-9 and Table

4-2). Therefore, the coverage in C_1 surface intermediates is essentially increasing with D_2/CO ratio (Fig.4-10) (the way we estimated θ is in Chapter 5). On the other hand, the coverage for C_2 and C_3 surface intermediates are decreasing. For C_2, the coverage decreases from 0.052 at $D_2/CO=1$ to 0.024 at $D_2/CO=6.54$. For C_3, the coverage decreases from 0.043 at $D_2/CO=1$ to 0.013 at $D_2/CO=6.54$.

When we add the coverage for C_1, C_2 and C_3, it emerges that this coverage is increasing with D_2/CO ratio. However, it can be seen that, for D_2/CO ratio from 1 to 6.54, even the largest value of the coverage (at $D_2/CO = 6.54$) is only around 0.26. Experiment invariantly shows that the coverage of CO does not change for the range of D_2/CO ratio (~ 1 ml/g). It is, therefore, envisaged that at a given temperature only a certain fraction of surface exposed-atoms participate in the chain growth for the range of D_2/CO ratio. An increase in D_2/CO ratio will enhance the coverage for C_1 and decrease the coverage for higher hydrocarbons. This phenomenon can be interpreted as the decreasing probability of forming higher hydrocarbons with increasing D_2/CO ratio.

Table 4-1: Average (area / τ_1) (A) for Species i and the Standard Deviation (σ)

Species	A	σ	σ/A,%
$^{13}C_2$	2.0568	0.1721	8.36
$^{12}C_1{}^{13}C_1$	0.9624	0.1783	18.52
$^{12}C_2$	0.8874	0.1456	16.41
$^{13}C_3$	2.9122	0.3082	10.58
$^{12}C_1{}^{13}C_2$	0.9476	0.1058	11.16
$^{12}C_2{}^{13}C_1$	0.5185	0.0393	7.59
$^{12}C_3$	1.1865	0.1454	12.25

*): with D_2/CO =3, T = 210°C, P = 1 atm.

**): Number of experiment = 5.

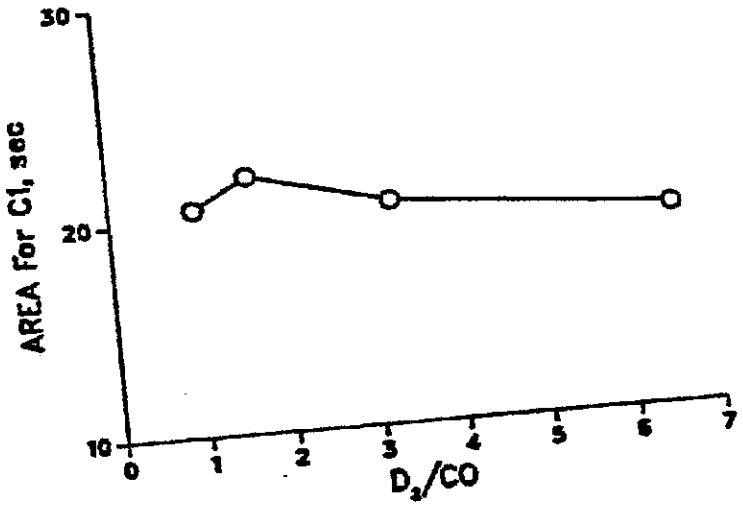

Figure 4-6: Transient Experiment over Co Catalyst
§5-1: The effect of D_2/CO ratio on areas for C_1

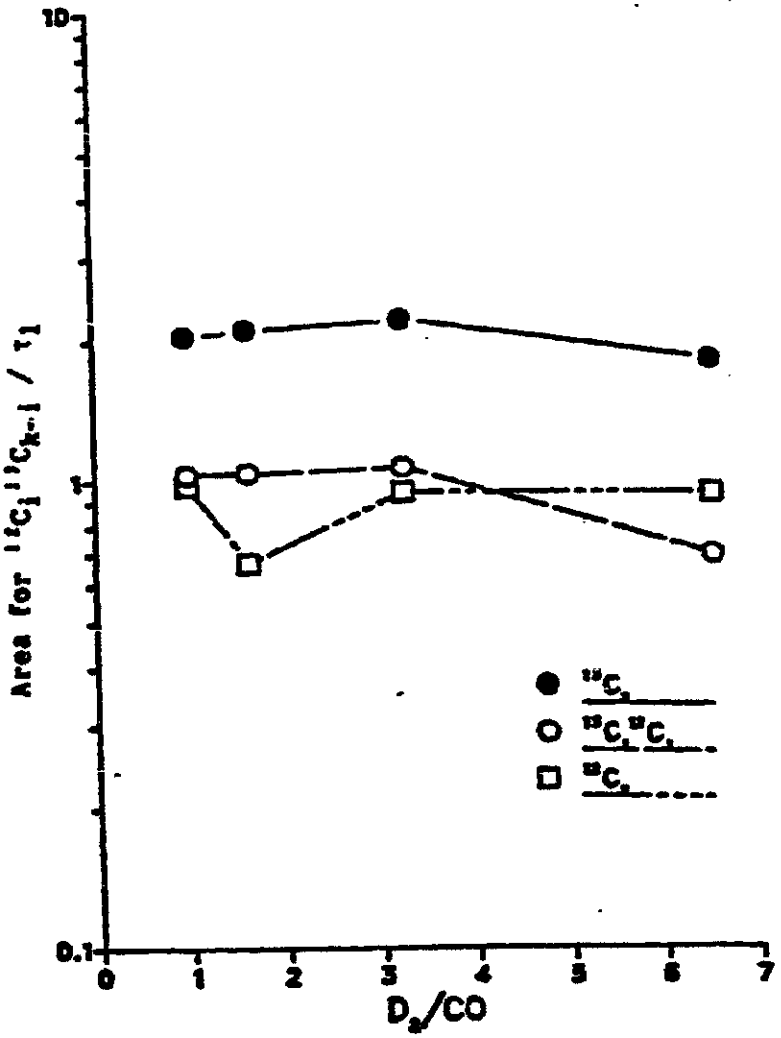

Figure 4-7: Transient Experiment over Co Catalyst
§5-2: The effect of D_2/CO ratio on areas for C_2

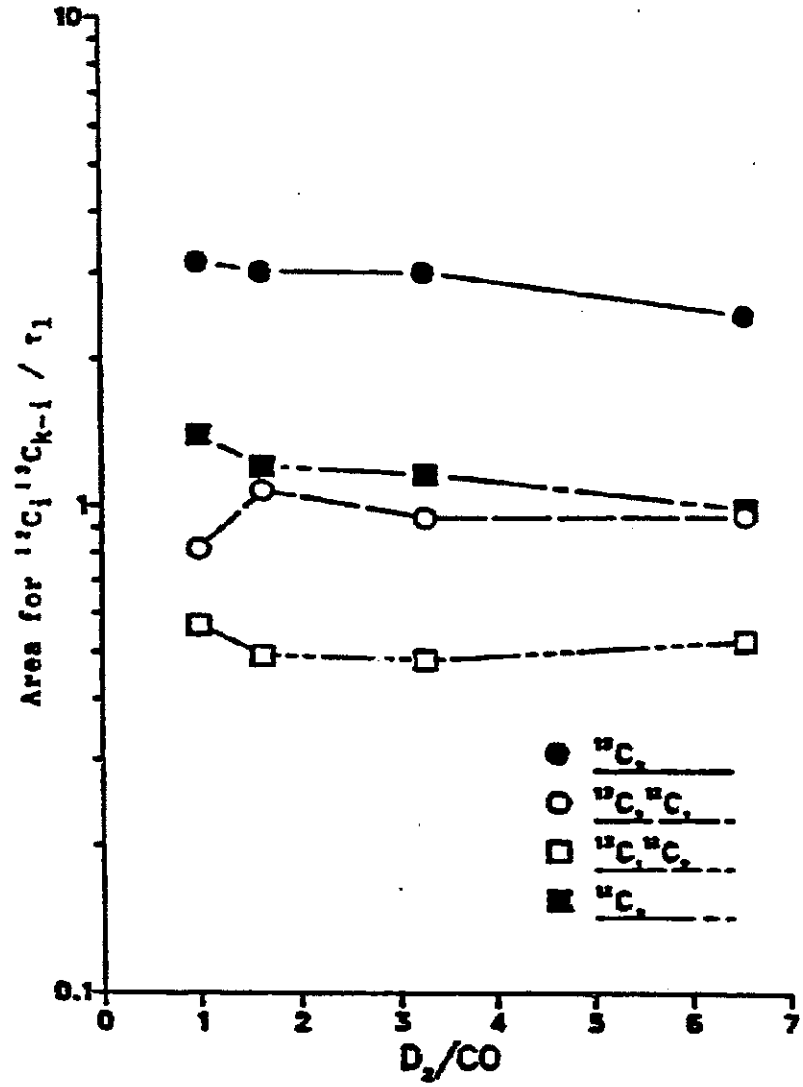

Figure 4-8: Transient Experiment over Co Catalyst
#5-3: The effect of D_2/CO ratio on areas for C_3

Table 4-2: TOF and α at Different D_2/CO Ratio

D_2/CO	1	1.636	3.273	6.545
$TOF_1 \times 10^{-3}, s^{-1}$	2.225	3.106	4.829	8.643
$TOF_2 \times 10^{-3}, s^{-1}$	1.763	1.679	1.575	1.328
$TOF_3 \times 10^{-3}, s^{-1}$	1.428	1.332	1.042	0.719
$TOF_t \times 10^{-3}, s^{-1}$	5.416	6.117	7.446	9.971
α	0.6501	0.6065	0.5204	0.4105

Note: TOF_i means TOF for C_i. TOF_t means the sum of TOF_i's.

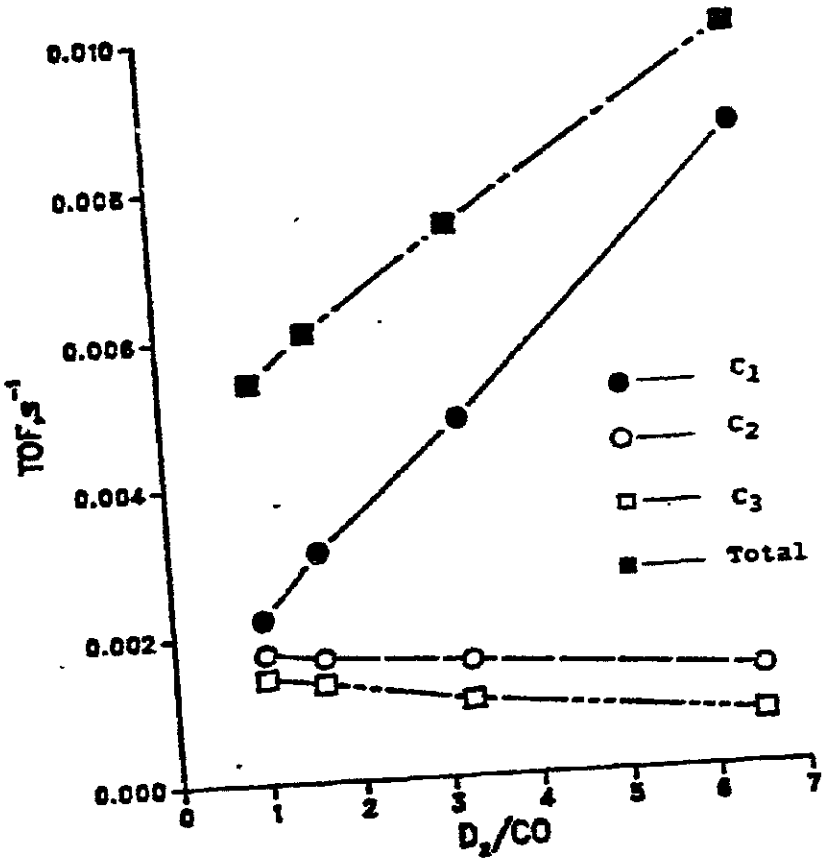

Figure 4-9: TOF for different D_2/CO Ratio

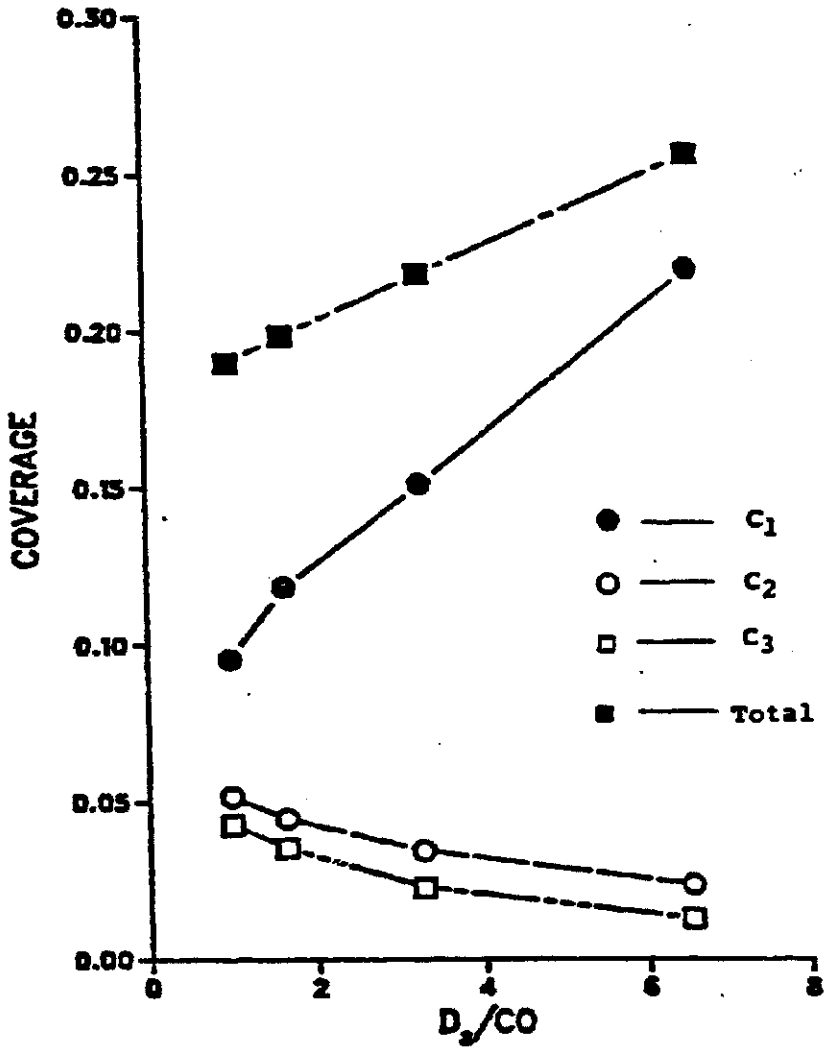

Figure 4-10: Transient Experiment over Co Catalyst #6: The effect of D_2/CO ratio on θ's